

Restoring the height of the terrain taking into account the statistical relationship of the interferometric pair of radar images

Oleg Goryachkin

Image Processing Systems Institute of RAS - Branch of the FSRC
"Crystallography and Photonics" RAS
Samara, Russia
oleg.goryachkin@gmail.com

Ivan Maslov

Image Processing Systems Institute of RAS - Branch of the FSRC
"Crystallography and Photonics" RAS
Samara, Russia
macloff@mail.ru

Abstract—An algorithm for reconstructing the height is proposed, which allows, based on the statistical relationship of the interferometric pair of radar images arising from the influence of the Earth's atmosphere, to clarify the height of the terrain. The results of numerical simulation are presented with the initial data corresponding to the parameters of the on-board equipment of the P-band bistatic radar system installed on the Aist-2D small spacecraft. The results obtained confirm the advisability of considering the statistical data on the state of the ionosphere in the algorithm of radar interferometry.

Keywords—height measurement error, ionosphere, P-band, radar imaging, radar interferometry, synthetic aperture radar.

I. INTRODUCTION

Currently, spacecraft equipped with synthetic aperture radar (SAR) allow you to receive radar (amplitude) images with high spatial resolution. However, SARs also make it possible to obtain phase information from reflecting objects and use it to reconstruct the third dimension, i.e. topographic elevation. The most developed frequency ranges are X-, C-, S- and L-bands. The launch of the next spacecraft with the P-band SAR of the Biomass of the European Space Agency is scheduled for 2021. The main difference between the P-range and the others used is high penetration and reflection stability. There are two main schemes for shooting images using SAR: monostatic when the transmitter and receiver are combined in space, and bistatic when the transmitter and receiver are separated in space. The placement of P-band monostatic SARs is complicated by well-known technical problems [1-4]: the destructive effect of the ionosphere, restrictions on the radio communication regulations, the need to use large antennas with a wide aperture, and a significant pulse power of the transmitter. So, for example, the basic design parameters of a BIOMASS spacecraft with a P-band monostatic SAR, suggest that the spatial resolution is not better than 50 m when using a 12-meter diameter antenna [5]. In [6–9], it was shown that multistatic (in particular bistatic, when the transmitter is placed on board the spacecraft and the receiving part on the Earth) radar observations open up the possibility of creating space-based radar sounding equipment in the P-bands of high-resolution. The need for a land-based stationary or mobile receiving station at a relatively short distance from the observed object limits the scope of application of such remote sensing systems. Nevertheless, it is possible to indicate some areas of application in which the proposed technologies have advantages: control of landscape changes; control of the ice situation around offshore oil and gas production platforms; precision farming; tactical intelligence; monitoring of forest resources, etc. The first in the history of remote sensing spaceborne radar system operating in the P-frequency range is a bistatic SAR installed on a small spacecraft Aist-2D.

Using the technology of multi-pass interferometric imaging, it is possible to restore the height of the terrain in the vicinity of the ground receiving point, and further control its change. The necessary interferometric base can be formed due to the special ballistic construction of the orbit of the spacecraft.

II. ALTITUDE RECOVERY ALGORITHM BASED ON ATMOSPHERIC STATISTICS

Consider the main stages of processing and obtaining a digital elevation model for the interferometric survey mode in a synthetic aperture radar (SAR):

1. The exact combination of two images (interferometric pair) obtained under the same conditions, but with a "small" diversity in space.
2. Finding the interferometric phase difference of the two images.
3. Filtering the resulting interferogram to reduce the influence of speckle noise.
4. Elimination of linear phase incursion in range.
5. The elimination of the ambiguity of the interferometric phase difference, which is due to the influence of the terrain.
6. Recalculation of the interferometric phase in the height of the terrain.
7. The procedure for geocoding.

Two images can be represented as:

$$\dot{I}_1 = \dot{f}_1(h)\dot{I}_{10} + \dot{n}_1 \quad \text{and} \quad \dot{I}_2 = \dot{f}_2(h)\dot{I}_{20} + \dot{n}_2, \quad (1)$$

where $\dot{f}_1(h) = \exp(-j\omega_0\tau'_{12}(0, x_0, y_0, 0)h)$ and $\dot{f}_2(h) = \exp(-j\omega_0\tau'_{22}(0, x_0, y_0, 0)h)$ functions describing the dependence of the height of the target, $\tau'_{12}(0, x_0, y_0, 0)$ and $\tau'_{22}(0, x_0, y_0, 0)$ - regular component signal delay, h - height, $\dot{I}_{10} = \sum_k \exp(-j\omega_0\delta_1(t_k))$ and $\dot{I}_{20} = \sum_k \exp(-j\omega_0\delta_2(t_k))$, $\delta_1(t_k)$ and $\delta_2(t_k)$ - a random component of the signal delay that occurs in the process of signal propagation in the Earth's atmosphere, \dot{n}_1 and \dot{n}_2 - independent additive complex noises in SAR channels.

An estimate of the maximum likelihood of the desired height under the conditions of known statistics of fluctuations in the time of arrival of a signal in the Earth's atmosphere can be written:

$$\begin{aligned}
 h &= \max_h p(\dot{I}_1, \dot{I}_2 | h) \\
 &= \max_h \iint_G p(\dot{I}_1, \dot{I}_2 | \dot{I}_{10}, \dot{I}_{20}, h) p(\dot{I}_{10}, \dot{I}_{20}) d\dot{I}_{10} d\dot{I}_{20}, \quad (2)
 \end{aligned}$$

where G is the region of integration on the complex plane,

$$\begin{aligned}
 p(I_1, I_2 | I_{10}, I_{20}, h) &= \frac{1}{2\pi\sigma_{n1}^2} \exp \left[-\frac{(\operatorname{Re}[I_1] - \operatorname{Re}[f_1(h)I_{10}])^2}{2\sigma_{n1}^2} \right. \\
 &\quad \left. - \frac{(\operatorname{Im}[I_1] - \operatorname{Im}[f_1(h)I_{10}])^2}{2\sigma_{n1}^2} \right] \\
 &\quad \times \frac{1}{2\pi\sigma_{n2}^2} \exp \left[-\frac{(\operatorname{Re}[I_2] - \operatorname{Re}[f_2(h)I_{20}])^2}{2\sigma_{n2}^2} \right. \\
 &\quad \left. - \frac{(\operatorname{Im}[I_2] - \operatorname{Im}[f_2(h)I_{20}])^2}{2\sigma_{n2}^2} \right],
 \end{aligned}$$

$\operatorname{Re}[I_1]$ and $\operatorname{Im}[I_1]$ - the real and imaginary part of the image \dot{I}_1 , $\operatorname{Re}[I_2]$ and $\operatorname{Im}[I_2]$ - the real and imaginary part of the image \dot{I}_2 , σ_{n1}^2 and σ_{n2}^2 - the noise variance of the first and second image.

We introduce the following notation: $\operatorname{Re}(I_1) = x_1$, $\operatorname{Im}(I_1) = y_1$; $\operatorname{Re}(I_2) = x_2$, $\operatorname{Im}(I_2) = y_2$; $\operatorname{Re}(I_{10}) = x_{10}$, $\operatorname{Im}(I_{10}) = y_{10}$; $\operatorname{Re}(I_{20}) = x_{20}$, $\operatorname{Im}(I_{20}) = y_{20}$; $\operatorname{Re}(f_1(h)) = k_{1x}$, $\operatorname{Im}(f_1(h)) = k_{1y}$; $\operatorname{Re}(f_2(h)) = k_{2x}$, $\operatorname{Im}(f_2(h)) = k_{2y}$.

Then

$$\begin{aligned}
 p(\dot{I}_{10}, \dot{I}_{20}) &= p(x_{10}, y_{10}, x_{20}, y_{20}) \\
 &= \frac{1}{\sigma_{\operatorname{Re}10} \sigma_{\operatorname{Im}10} \sigma_{\operatorname{Re}20} \sigma_{\operatorname{Im}20} \sqrt{(2\pi)^4 \operatorname{Det}}} \exp \left\{ -\frac{1}{2\operatorname{Det}} \left[D_{11} \frac{x_{10}^2}{\sigma_{\operatorname{Re}10}^2} \right. \right. \\
 &+ D_{12} \frac{x_{10} y_{10}}{\sigma_{\operatorname{Re}10} \sigma_{\operatorname{Im}10}} + D_{13} \frac{x_{10} x_{20}}{\sigma_{\operatorname{Re}10} \sigma_{\operatorname{Re}20}} + D_{14} \frac{x_{10} y_{20}}{\sigma_{\operatorname{Re}10} \sigma_{\operatorname{Im}20}} \\
 &+ D_{21} \frac{y_{10} x_{10}}{\sigma_{\operatorname{Re}10} \sigma_{\operatorname{Im}10}} + D_{22} \frac{y_{10}^2}{\sigma_{\operatorname{Im}10}^2} + D_{23} \frac{y_{10} x_{20}}{\sigma_{\operatorname{Im}10} \sigma_{\operatorname{Re}20}} \\
 &+ D_{24} \frac{y_{10} y_{20}}{\sigma_{\operatorname{Im}10} \sigma_{\operatorname{Im}20}} + D_{31} \frac{x_{20} x_{10}}{\sigma_{\operatorname{Re}20} \sigma_{\operatorname{Re}10}} + D_{32} \frac{x_{20} y_{10}}{\sigma_{\operatorname{Re}20} \sigma_{\operatorname{Im}10}} \\
 &+ D_{33} \frac{x_{20}^2}{\sigma_{\operatorname{Re}20}^2} + D_{34} \frac{x_{20} y_{20}}{\sigma_{\operatorname{Re}20} \sigma_{\operatorname{Im}20}} + D_{41} \frac{y_{20} x_{10}}{\sigma_{\operatorname{Im}20} \sigma_{\operatorname{Re}10}} \\
 &\left. \left. + D_{42} \frac{y_{20} y_{10}}{\sigma_{\operatorname{Im}20} \sigma_{\operatorname{Im}10}} + D_{43} \frac{y_{20} x_{20}}{\sigma_{\operatorname{Im}20} \sigma_{\operatorname{Re}20}} + D_{44} \frac{y_{20}^2}{\sigma_{\operatorname{Im}20}^2} \right\}, \quad (3)
 \end{aligned}$$

where Det - is the determinant of the correlation matrix $p(\operatorname{Re}(I_{10}), \operatorname{Im}(I_{10}), \operatorname{Re}(I_{20}), \operatorname{Im}(I_{20}))$, D_{ij} - is the algebraic complement of the element R_{ij} in the determinant Det .

After simplification, we write the multidimensional probability density for the quantities $x_{10}, y_{10}, x_{20}, y_{20}$:

$$\begin{aligned}
 p(I_{10}, I_{20}) &= \frac{1}{4\pi^2 \sigma_{\operatorname{Re}10} \sigma_{\operatorname{Im}10} \sigma_{\operatorname{Re}20} \sigma_{\operatorname{Im}20} \sqrt{\operatorname{Det}}} \\
 &\times \exp \left\{ -\frac{1}{2\operatorname{Det}} \left[D_{11} \frac{(x_{10} - M_0)^2}{\sigma_{\operatorname{Re}10}^2} + D_{33} \frac{(x_{20} - M_0)^2}{\sigma_{\operatorname{Re}20}^2} \right. \right. \\
 &+ D_{22} \frac{y_{10}^2}{\sigma_{\operatorname{Im}10}^2} + (D_{13} + D_{31}) \frac{(x_{10} - M_0)(x_{20} - M_0)}{\sigma_{\operatorname{Re}10} \sigma_{\operatorname{Re}20}} \\
 &\left. \left. + D_{44} \frac{y_{20}^2}{\sigma_{\operatorname{Im}20}^2} + (D_{24} + D_{42}) \frac{y_{20} y_{10}}{\sigma_{\operatorname{Im}20} \sigma_{\operatorname{Im}10}} \right] \right\}, \quad (4)
 \end{aligned}$$

where $\sigma_{\operatorname{Re}10}$, $\sigma_{\operatorname{Im}10}$, $\sigma_{\operatorname{Re}20}$, $\sigma_{\operatorname{Im}20}$ - are the standard deviations of the real and imaginary parts of the first and second images, respectively, and algebraic additions.

We find the height estimate by integrating analytically.

$$\begin{aligned}
 h &= \max_h p(I_1, I_2 | h) \\
 &= \max_h \iint p(I_1, I_2 | I_{10}, I_{20}, h) p(I_{10}, I_{20}) dI_{10} dI_{20} \\
 &= \max_h p(x_1, y_1, x_2, y_2 | h) \\
 &= \max_h \iiint p(x_1, y_1, x_2, y_2 | x_{10}, y_{10}, x_{20}, y_{20}, h) \\
 &\quad \times p(x_{10}, y_{10}, x_{20}, y_{20}) dx_{10} dy_{10} dx_{20} dy_{20} \quad (5)
 \end{aligned}$$

1. Simplify $p(x_1, y_1, x_2, y_2 | x_{10}, y_{10}, x_{20}, y_{20}, h)$.

$$\begin{aligned}
 p(I_1, I_2 | I_{10}, I_{20}, h) &= \frac{1}{4\pi^2 D_n^2} \exp \left\{ -\frac{1}{2} \left[\frac{x_1^2 + y_1^2 + x_2^2 + y_2^2}{D_n} \right] \right\} \\
 &\times \exp \left\{ -\frac{1}{2} \left[\frac{1}{D_n} x_{10}^2 + \frac{1}{D_n} y_{10}^2 + \frac{1}{D_n} x_{20}^2 + \frac{1}{D_n} y_{20}^2 \right. \right. \\
 &\quad - \frac{(2k_{1x} x_1 + 2k_{1y} y_1)}{D_n} x_{10} + \frac{(-2k_{1x} y_1 + 2k_{1y} x_1)}{D_n} y_{10} \\
 &\quad \left. \left. - \frac{(2k_{2x} x_2 + 2k_{2y} y_2)}{D_n} x_{20} + \frac{(-2k_{2x} y_2 + 2k_{2y} x_2)}{D_n} y_{20} \right] \right\}, \quad (6)
 \end{aligned}$$

where $D_n = \sigma_{n1}^2 = \sigma_{n2}^2$.

2. Simplify $p(x_{10}, y_{10}, x_{20}, y_{20})$.

$$\begin{aligned}
 p(x_{10}, y_{10}, x_{20}, y_{20}) &= \frac{1}{\sigma_{\operatorname{Re}10} \sigma_{\operatorname{Im}10} \sigma_{\operatorname{Re}20} \sigma_{\operatorname{Im}20} 4\pi^2 \sqrt{\operatorname{Det}}} \\
 &\times \exp \left\{ -\frac{1}{2\operatorname{Det}} \left[\frac{D_{11} M_0^2}{\sigma_{\operatorname{Re}10}^2} + \frac{D_{33} M_0^2}{\sigma_{\operatorname{Re}20}^2} + \frac{(D_{13} + D_{31}) M_0^2}{\sigma_{\operatorname{Re}10} \sigma_{\operatorname{Re}20}} \right] \right\} \\
 &\times \exp \left\{ -\frac{1}{2\operatorname{Det}} \left[\frac{D_{11}}{\sigma_{\operatorname{Re}10}^2} x_{10}^2 + \frac{D_{22}}{\sigma_{\operatorname{Im}10}^2} y_{10}^2 + \frac{D_{33}}{\sigma_{\operatorname{Re}20}^2} x_{20}^2 + \frac{D_{44}}{\sigma_{\operatorname{Im}20}^2} y_{20}^2 \right. \right. \\
 &+ \frac{(D_{13} + D_{31})}{\sigma_{\operatorname{Re}10} \sigma_{\operatorname{Re}20}} x_{10} x_{20} - \left[\frac{2M_0 D_{11}}{\sigma_{\operatorname{Re}10}^2} + \frac{(D_{13} + D_{31}) M_0}{\sigma_{\operatorname{Re}10} \sigma_{\operatorname{Re}20}} \right] x_{10} \\
 &\left. \left. - \left[\frac{2M_0 D_{33}}{\sigma_{\operatorname{Re}20}^2} + \frac{(D_{13} + D_{31}) M_0}{\sigma_{\operatorname{Re}10} \sigma_{\operatorname{Re}20}} \right] x_{20} + \frac{(D_{24} + D_{42})}{\sigma_{\operatorname{Im}10} \sigma_{\operatorname{Im}20}} y_{10} y_{20} \right] \right\} \quad (7)
 \end{aligned}$$

3. We write $p(x_1, y_1, x_2, y_2 | h)$ down considering the above transformations.

$$\begin{aligned}
 p(x_1, y_1, x_2, y_2 | h) &= \frac{1}{16\pi^4 D_n^2 \sigma_{Re10} \sigma_{Im10} \sigma_{Re20} \sigma_{Im20} \sqrt{Det}} \\
 &\times \exp \left\{ -\frac{1}{2} \left[\frac{x_1^2 + y_1^2 + x_2^2 + y_2^2}{D_n} + \frac{D_{11} M_0^2}{\sigma_{Re10}^2 Det} + \frac{D_{33} M_0^2}{\sigma_{Re20}^2 Det} \right. \right. \\
 &+ \left. \left. \frac{(D_{13} + D_{31})}{\sigma_{Re10} \sigma_{Re20} Det} M_0^2 \right] \right\} \iiint \exp \left\{ -\frac{1}{2} \left[\left(\frac{1}{D_n} + \frac{D_{11}}{\sigma_{Re10}^2 Det} \right) x_{10}^2 \right. \right. \\
 &+ \left. \left(\frac{1}{D_n} + \frac{D_{22}}{\sigma_{Im10}^2 Det} \right) y_{10}^2 + \left(\frac{1}{D_n} + \frac{D_{33}}{\sigma_{Re20}^2 Det} \right) x_{20}^2 \right. \\
 &- \left. \left(\frac{(2k_{1x} x_1 + 2k_{1y} y_1)}{D_n} + \frac{2M_0 D_{11}}{\sigma_{Re10}^2 Det} + \frac{(D_{13} + D_{31}) M_0}{\sigma_{Re10} \sigma_{Re20} Det} \right) x_{10} \right. \\
 &+ \left. \frac{(-2k_{1x} y_1 + 2k_{1y} x_1)}{D_n} y_{10} + \frac{(-2k_{2x} y_2 + 2k_{2y} x_2)}{D_n} y_{20} \right. \\
 &+ \left. \frac{(D_{13} + D_{31})}{\sigma_{Re10} \sigma_{Re20} Det} x_{10} x_{20} + \left(\frac{1}{D_n} + \frac{D_{44}}{\sigma_{Im20}^2 Det} \right) y_{20}^2 \right. \\
 &- \left. \left(\frac{(2k_{2x} x_2 + 2k_{2y} y_2)}{D_n} + \frac{2M_0 D_{33}}{\sigma_{Re20}^2 Det} + \frac{(D_{13} + D_{31}) M_0}{\sigma_{Re10} \sigma_{Re20} Det} \right) x_{20} \right. \\
 &+ \left. \left. \frac{(D_{24} + D_{42})}{\sigma_{Im10} \sigma_{Im20} Det} y_{10} y_{20} \right] \right\} dx_{10} dy_{10} dx_{20} dy_{20} \quad (8)
 \end{aligned}$$

We calculate the resulting integral.

As you can see, it is a multidimensional probability density of a combination of random variables, then

$$\frac{1}{\sqrt{(2\pi)^n \det B^{-1}}} \int \dots \int \exp \left\{ -\frac{1}{2} (\bar{x} - \bar{a})^T B (\bar{x} - \bar{a}) \right\} d\bar{x} = 1, \quad (9)$$

where $\bar{x} = \begin{bmatrix} x_{10} \\ y_{10} \\ x_{20} \\ y_{20} \end{bmatrix}$, \bar{a} is the vector of mean values, B is the covariance matrix.

Since the matrix B is symmetric, we can write:

$$\begin{aligned}
 (\bar{x} - \bar{a})^T B (\bar{x} - \bar{a}) &= \bar{x}^T B \bar{x} - 2\bar{a}^T B \bar{x} + \bar{a}^T B \bar{a} \\
 &= \bar{x}^T B \bar{x} - C \bar{x} + D, \quad (10)
 \end{aligned}$$

where $C = 2\bar{a}^T B \Rightarrow a^T = \frac{1}{2} B^{-1} C$ then

$$D = a^T B a = \frac{1}{4} C B^{-1} B (C B^{-1})^T = \frac{1}{4} C B^{-1} C^T.$$

We will receive

$$\int \dots \int \exp \left\{ -\frac{1}{2} (\bar{x}^T B \bar{x} - C \bar{x}) \right\} d\bar{x} = \sqrt{(2\pi)^n \frac{1}{\det B}} \exp \left\{ \frac{1}{2} D \right\}.$$

Define a vector C :

$$C = \begin{bmatrix} - \left(\frac{(2k_{1x} x_1 + 2k_{1y} y_1)}{D_n} + \frac{2M_0 D_{11}}{\sigma_{Re10}^2 Det} + \frac{(D_{13} + D_{31}) M_0}{\sigma_{Re10} \sigma_{Re20} Det} \right) \\ \frac{(-2k_{1x} y_1 + 2k_{1y} x_1)}{D_n} \\ - \left(\frac{(2k_{2x} x_2 + 2k_{2y} y_2)}{D_n} + \frac{2M_0 D_{33}}{\sigma_{Re20}^2 Det} + \frac{(D_{13} + D_{31}) M_0}{\sigma_{Re10} \sigma_{Re20} Det} \right) \\ \frac{(-2k_{2x} y_2 + 2k_{2y} x_2)}{D_n} \end{bmatrix} \quad (11)$$

Define the matrix B :

$$B = \begin{bmatrix} b_{11} & 0 & b_{13} & 0 \\ 0 & b_{22} & 0 & b_{24} \\ b_{31} & 0 & b_{33} & 0 \\ 0 & b_{42} & 0 & b_{44} \end{bmatrix}, \quad (12)$$

where $b_{11} = \left(\frac{1}{D_n} + \frac{D_{11}}{\sigma_{Re10}^2 Det} \right)$, $b_{22} = \left(\frac{1}{D_n} + \frac{D_{22}}{\sigma_{Im10}^2 Det} \right)$,

$b_{33} = \left(\frac{1}{D_n} + \frac{D_{33}}{\sigma_{Re20}^2 Det} \right)$, $b_{44} = \left(\frac{1}{D_n} + \frac{D_{44}}{\sigma_{Im20}^2 Det} \right)$,

$b_{13} = b_{31} = \frac{(D_{13} + D_{31})}{\sigma_{Re10} \sigma_{Re20} Det}$, $b_{24} = b_{42} = \frac{(D_{24} + D_{42})}{\sigma_{Im10} \sigma_{Im20} Det}$.

We write

$$\begin{aligned}
 p(I_1, I_2 | h) &= \frac{1}{16\pi^4 D_n^2 \sigma_{Re10} \sigma_{Im10} \sigma_{Re20} \sigma_{Im20} \sqrt{Det}} \\
 &\times \exp \left\{ -\frac{1}{2} \left[\frac{x_1^2 + y_1^2 + x_2^2 + y_2^2}{D_n} + \frac{D_{11} M_0^2}{\sigma_{Re10}^2 Det} \right. \right. \\
 &+ \left. \frac{D_{33} M_0^2}{\sigma_{Re20}^2 Det} + \frac{(D_{13} + D_{31})}{\sigma_{Re10} \sigma_{Re20} Det} M_0^2 \right] \left. \right\} \\
 &\times \iiint \exp \left\{ -\frac{1}{2} [\bar{x}^T B \bar{x} - C \bar{x}] \right\} d\bar{x} \quad (13)
 \end{aligned}$$

Finally, we obtain an algorithm for estimating the height of the terrain, considering the random nature of signal propagation in the Earth's atmosphere in a form that does not contain multiple integrals:

$$\begin{aligned}
 h &= \max_h p(x_1, y_1, x_2, y_2 | h) \\
 &= \frac{1}{4\pi^2 D_n^2 \sigma_{Re10} \sigma_{Im10} \sigma_{Re20} \sigma_{Im20} \sqrt{Det} \sqrt{\det B}} \\
 &\times \exp \left\{ \frac{1}{2} D - \frac{1}{2} \left[\frac{x_1^2 + y_1^2 + x_2^2 + y_2^2}{D_n} + \frac{D_{11} M_0^2}{\sigma_{Re10}^2 Det} \right. \right. \\
 &+ \left. \frac{D_{33} M_0^2}{\sigma_{Re20}^2 Det} + \frac{(D_{13} + D_{31})}{\sigma_{Re10} \sigma_{Re20} Det} M_0^2 \right] \left. \right\}. \quad (14)
 \end{aligned}$$

The main question that arises in this case is the advisability of considering the atmosphere in the algorithm for determining altitude. Will there be a gain in the correct accounting of the statistical model of the atmosphere. To answer this question, mathematical modeling was carried out.

III. MATHEMATICAL MODELING RESULTS

Figure 1 show the results of calculations for different values of the true correlation coefficient with the following initial data:

- signal to noise ratio 23 dB
- interferometric base 10 km.
- the angle of inclination of the base is zero degrees.
- angle of sight 45 degrees.

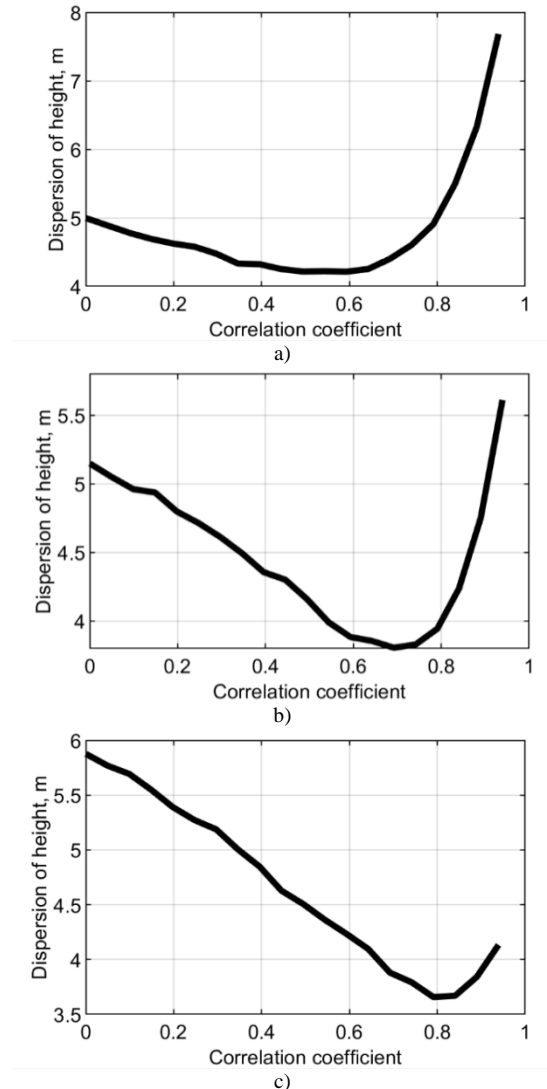


Fig. 1. The true value of the correlation coefficient is 0.7 (a), 0.8 (b) and 0.9 (c), respectively.

IV. CONCLUSION

From the data obtained it follows that the greater the correlation coefficients between the real and imaginary parts of two images (interferometric pair), the greater the value of the gain from the application of the proposed algorithm, considering statistical data on the state of the ionosphere.

REFERENCES

- [1] A. Ishimaru, Y. Kuga, J. Liu, Y. Kim and T. Freeman, "Ionospheric effects on synthetic aperture radar at 100 MHz to 2 GHz," *Radio Science (USA)*, vol. 34, no. 1, pp. 257-268, 1999.
- [2] O.V. Goriachkin and D.D. Klovsy, "The some problems of realization spaceborne SAR's in P,UHF,VHF bands," *Proceedings IEEE International Geoscience and Remote Sensing Symposium, Hamburg, Germany*, vol. 2, pp. 1271-1273, 1999.
- [3] O.V. Goriachkin, "The effect of the Earth's atmosphere on the degradation of the characteristics of images of synthetic aperture space-based radars," *Computer Optics*, vol. 24, pp. 177-183, 2002.
- [4] O.V. Goriachkin, "Blind signal processing methods and their applications in radio engineering and communication systems," *M.: Radio and communication*, 2003, 230 p.
- [5] T. Fügen, E. Sperlich, C. Heer, S. Riegger, C. Warren, A. Carbone and F. Hélière, "The Biomass SAR Instrument: Development Status and Performance Overview," *IEEE International Geoscience and Remote Sensing Symposium*, pp. 8571-8574, 2018.
- [6] O.V. Goriachkin, "Ways of the development of the radar space systems of the remot sensing of the Earth," *Vestnik of Samara University*, vol. 2, pp. 92-104, 2010.
- [7] O.V. Goriachkin, B.G. Zhengurov, V.B. Bakeev, A.Yu. Baraboshin, A.V. Nevsky and E.G. Skorobogatov, "Synthetic P-band aperture bistatic radar for Aits-2D small spacecraft," *Electrosvyaz magazine*, vol. 8, pp. 34-39, 2015.
- [8] O.V. Goriachkin, A.V. Borisenkov and B.G. Zhengurov, "Imaging in ground-based P band bistatic SAR," *Radioengineering*, vol. 1, pp. 117-121, 2017.
- [9] A.N. Kirilin, R.N. Akhmetov, E.V. Shakhmatov, S.I. Tkachenko, A.I. Baklanov, V.V. Salmin, N.D. Semkin, I.S. Tkachenko and O.V. Goriachkin, "Experimental and technological small spacecraft AIST-2D," *Samara: Publishing House of SamSC RAS*, 2017, 324 p.